Poster presentation | Poster session
Poster Session
Thu. Jul 18, 2024 4:30 PM - 6:30 PM Room P

# [PO-10] Comparison of the high-order Runge-Kutta discontinuous Galerkin method and gas-kinetic scheme for inviscid compressible flow simulations

*Yixiao Wang[1], Xing Ji[1], Gang Chen[1] （1. Xi'an Jiaotong University）

Keywords: discontinuous Galerkin, compact GKS, conservation laws

**Twelfth International Conference on Computational Fluid Dynamics (ICCFD12), Kobe, Japan, July 14-19, 2024**

**ICCFD12-2024-C000284**

# Comparison of the high-order Runge-Kutta discontinuous Galerkin method and gas-kinetic scheme for inviscid compressible flow simulations

Y.X.Wang*, X. Ji* , G. Chen*
Corresponding author: xjiad@connect.ust.hk
* Xian Jiaotong University, Xian, 710049, China.

**Abstract:** In this work, we systematically investigate the performance of the Runge-Kutta discontinuous Galerkin(RKDG) method with different numerical fluxes and the gas-kinetic scheme(GKS) with both compact and noncompact spatial reconstruction. Accuracy, efficiency and shock-capturing capabilities are all within our comparison range. It can be concluded that the compact GKS(CGKS) has similar efficiency performance in smooth region as RKDG method in the same spatial order but capture shock waves more precisely and robustly.

*Keywords:* discontinuous Galerkin, compact GKS, conservation laws

## 1 Introduction

Both the RKDG method and GKS have abilities to solve the nonlinear time-dependent hyperbolic conservation laws. In the work of recent years, the RKDG method with multi-resolution limiters [1] as well as the GKS with compact spatial reconstruction(CGKS) [2] have great performance for simulating flows efficiently.

The primary differences between the RKDG method and the GKS are outlined as follows:
1. CFL Number Flexibility: GKS operates with fewer restrictions on the Courant-Friedrichs-Lewy (CFL) number compared to RKDG. However, reaching the accuracy level of RKDG or other high-order schemes can be challenging for GKS, mainly due to the constraints imposed by its finite volume framework.
2. Identification of Troubled Cells and Limiting: RKDG and GKS use markedly different approaches for detecting troubled cells and applying limits to the numerical solution. These differences stem from their unique ways of handling the evolution of degrees of freedom within each cell.
3. Mathematical Formulation and Physical Foundation: RKDG is known for its straightforward mathematical formulation, though its performance can be problematic in regions with strong discontinuities, where robustness tends to deteriorate quickly. In contrast, GKS, while more complex in formulation and less straightforward to extend to very high orders, is rooted in a physical model of gas dynamics [3], offering enhanced flexibility for managing complex flow scenarios.
4. Degrees of Freedom and Computational Demands: RKDG allows for high accuracy with limited mesh refinement due to ample degrees of freedom. However, increasing the order of the scheme typically reduces the permissible time step size, demanding greater memory bandwidth. On the other hand, the CGKS may have fewer degrees of freedom but achieves high-order accuracy through spatial reconstruction. Its spatio-temporal coupling approach relaxes CFL conditions for time advancement, although the computation of time-accurate gas-kinetic flux terms can reduce its overall efficiency.

In this research, we address the solutions of one- and two-dimensional nonlinear hyperbolic conservation laws using the Runge-Kutta Discontinuous Galerkin (RKDG) method and the Gas-Kinetic Scheme (GKS), evaluating their performance across various standard test cases.

## 2 Current Numerical Results

### 2.1 One dimensional accuracy tests

In this subsection, one dimensional advection of density perturbation is tested, and the initial condition is given as follows

$$\rho(x) = 1 + 0.2\sin(\pi x), \quad U(x) = 1, \quad p(x) = 1, x \in [-1, 1].$$

With the periodic boundary condition, and the analytic solution is

$$\rho(x,t) = 1 + 0.2\sin(\pi(x-t)), \quad U(x,t) = 1, \quad p(x,t) = 1.$$

In this computation, the computational domain is partitioned by uniform meshes, and the final time is $t = 2s$. And the classical fourth-order Runge-Kutta method [4] is adopted for RKDG-$P^4$ method to guarantee that the spatial error dominates. We measure the efficiency of the two methods using the CPU time calculated from the $L^1$ and $L^2$ errors, which is shown in Figure 1 and Figure 2.

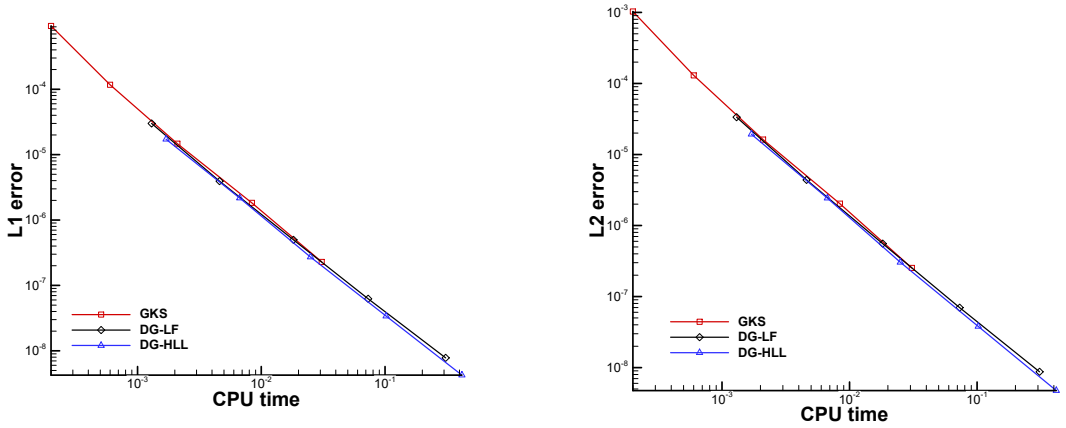


Figure 1: Efficiency of simulation for smooth regions: comparisons between RKDG-$P^2$ method and third-order GKS method. The left one is based on $L^1$ error and the right one is based on $L^2$ error.

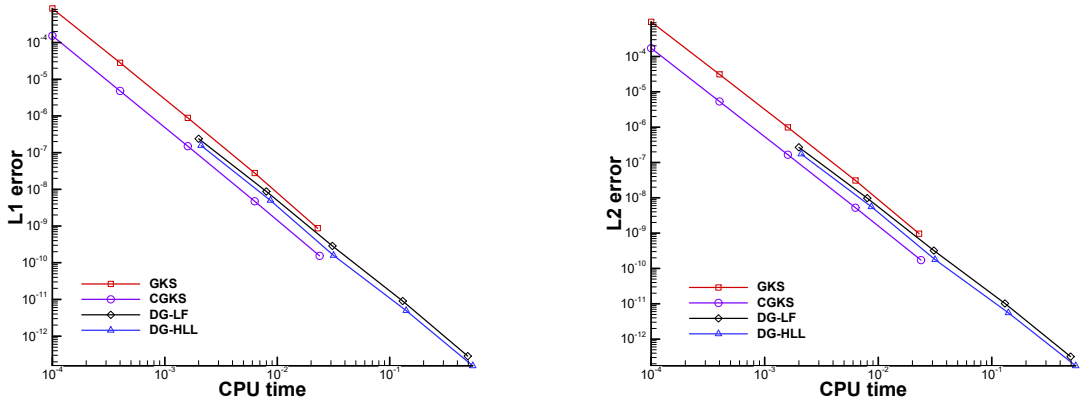


Figure 2: Efficiency of simulation for smooth regions: comparisons between RKDG-$P^4$ and fifth-order GKS and CGKS. The left one is based on $L^1$ error and the right one is based on $L^2$ error.

## 2.2 One dimensional problems with discontinuities

In this subsection, we present several numerical tests with discontinuities in one dimension.

The first case is the Shu-Osher problem [5], which is used to test the performance of the numerical methods in a domain consisting of both shocks and complex smooth regions. The initial conditions are

$$(\rho, U, p) = \begin{cases} (3.857134, 2.629369, 10.33333), & -5 < x \leq -4, \\ (1 + 0.2\sin(5x), 0, 1), & -4 < x < 5, \end{cases}$$

and the computational domain is (-5,5). The density distributions at $t = 1.8s$ of the two methods against reference solution computed by the fifth-order WENO scheme with 10000 grid points are shown in Figure 3.

As an extension of the Shu-Osher problem, the Titarev-Toro problem [6] is tested as well, and the initial conditions in this case are the following

$$(\rho, U, p) = \begin{cases} (1.515695, 0.523346, 1.805), & -5 < x \leq -4.5, \\ (1 + 0.1\sin(20\pi x), 0, 1), & -4.5 < x < 5, \end{cases}$$

and the computational domain is (-5,5). The non-reflecting boundary condition is imposed on left end, and the fixed wave profile is given on the right end in the two cases. The results of the two methods together with the reference solution is computed by fifth-order WENO scheme with 10000 grids are shown in Figure 4. As the results of the accuracy test, the performance of the RKDG method for simulating complex structure with shock waves and acoustic waves is between GKS and CGKS.

The last case for one-dimensional problems is the double rarefaction wave problem [7]. The initial conditions are

$$(\rho, U, p) = \begin{cases} (1, -2, 0.4), & 0 < x \leq 0.5, \\ (1, 2, 0.4), & 0.5 < x < 1, \end{cases} \tag{1}$$

and the computational domain is (0,1). The case is hard to simulate because of the near-vacuum region in the middle of domain. The results of the two methods together with exact solution computed by the exact Riemann solver [8] are shown in Figure 5.

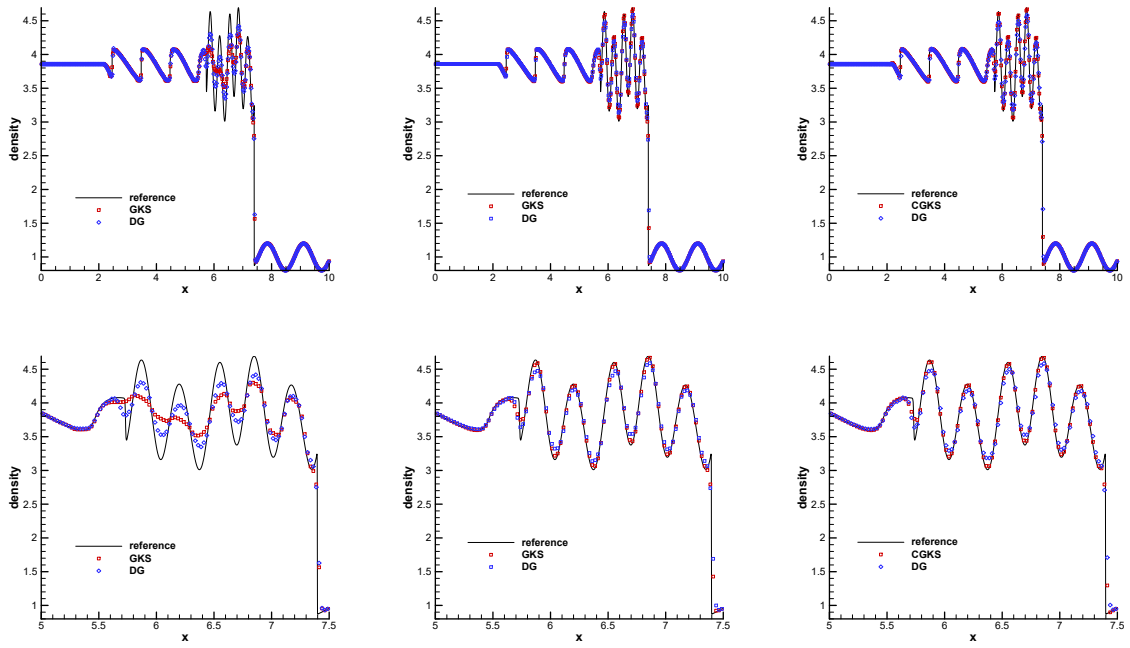


Figure 3: Shu-Osher problem: the density distributions and local enlargement at $t = 1.8s$ with 400 cells. Left to right: RKDG-$P^2$ with third-order GKS, RKDG-$P^4$ with fifth-order GKS, RKDG-$P^4$ with fifth-order CGKS.

## 2.3 Two dimensinal accuracy test

In this subsection, two dimensional advection of density perturbation is tested, and the initial condition is given as follows

$$\rho(x, y) = 1 + 0.2\sin(\pi(x + y)), \quad U(x, y) = 1, \quad V(x, y) = 1, \quad p(x, y) = 1, x, y \in [-1, 1].$$

With the periodic boundary condition, and the analytic solution is

$$\rho(x, y, t) = 1 + 0.2\sin(\pi(x + y - t)), \quad U(x, y, t) = 1, \quad V(x, y, t) = 1, \quad p(x, y, t) = 1.$$

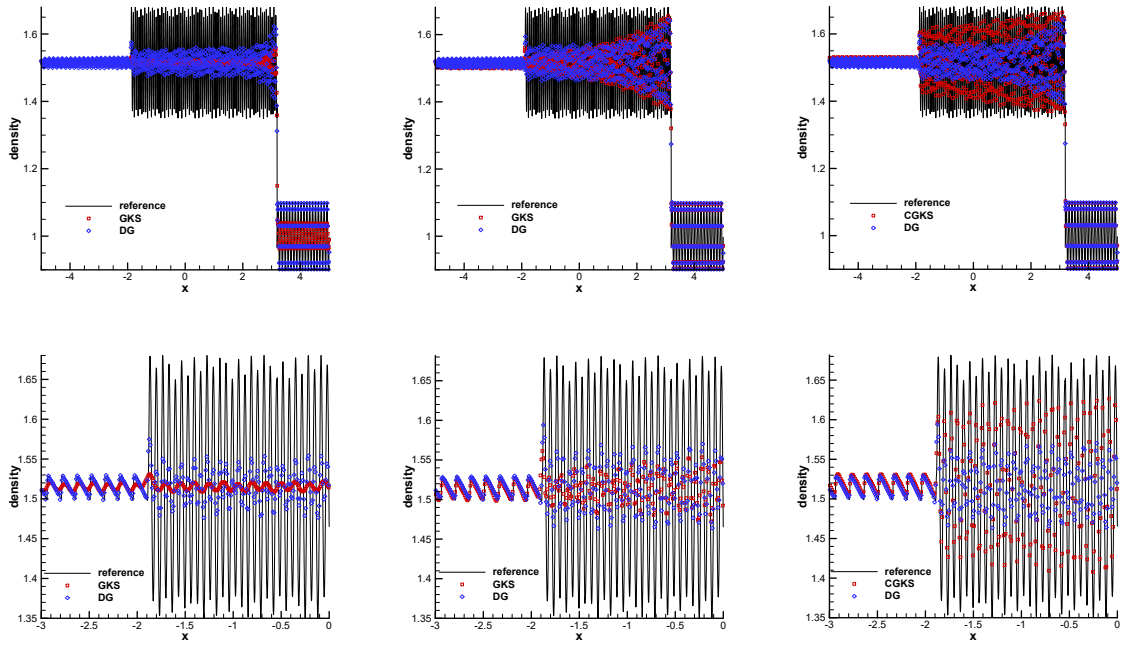


Figure 4: Titarev-Toro problem: the density distributions and local enlargement at $t = 5s$ with 1000 cells. Left to right: RKDG-$P^2$ with third-order GKS, RKDG-$P^4$ with fifth-order GKS, RKDG-$P^4$ with fifth-order CGKS.

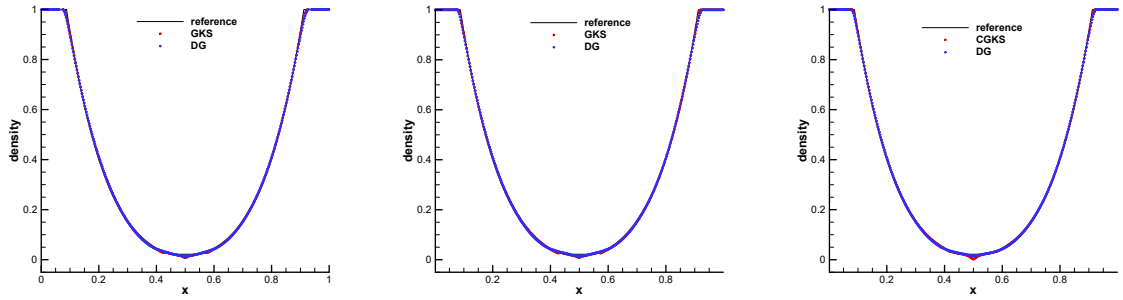


Figure 5: Double rarefaction waves: the density distributions and local enlargement at $t = 0.15s$ with 400 cells. Left to right: RKDG-$P^2$ with third-order GKS, RKDG-$P^4$ with fifth-order GKS, RKDG-$P^4$ with fifth-order CGKS.

The simulation time is $t = 2s$ in this case. And fourth-order Runge-Kutta method [4] is adopted for RKDG-$P^4$ to guarantee that the spatial error dominates. The comparison of the efficiency is presented in Figure 6.

## 2.4 Double Mach reflection problem

This problem was extensively studied by Woodward and Colella [9] for the inviscid flow. The computational domain is $[0, 4] \times [0, 1]$, and a solid wall lies at the bottom of the computational domain starting from $x = 1/6$. Initially, a right-moving Mach 10 shock is positioned at $(x, y) = (1/6, 0)$, and makes a $60^\circ$ angle with the x-axis. The initial pre-shock and post-shock conditions are

$$(\rho, U, V, p) = (8, 4.125\sqrt{3}, -4.125, 116.5),$$
$$(\rho, U, V, p) = (1.4, 0, 0, 1).$$

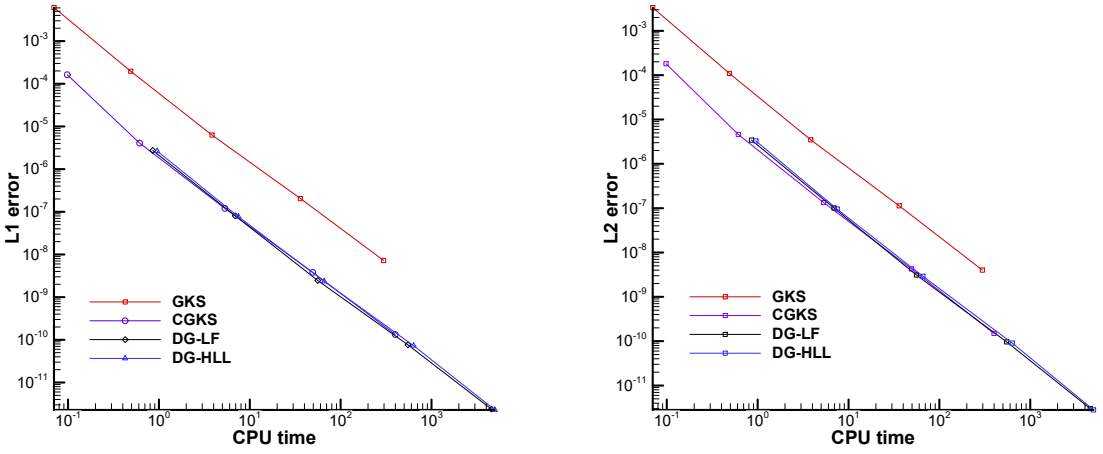


Figure 6: Efficiency of simulation for two dimensional smooth regions:comparisons between RKDG-$P^4$ method and fifth-order GKS/CGKS method. The left one is based on $L^1$ error and the right one is based on $L^2$ error

.

In this case, we tend to compare the resolution of the two methods under the premise of almost the same computational load. A baseline uniform mesh with $800 \times 200$ grid points is used for the two methods, and a refined one ($1600 \times 400$) is used in the CGKS method to make the comparison fair. There are 15 degrees of freedom contained in a single cell in the RKDG-$P4$ method, but only one and three degrees of freedom for each variable in the GKS and CGKS, respectively. Thus, the refined one has similar degrees of freedom($1,920,000$ totally) with the RKDG-$P4$ method($2,400,000$ totally). As is shown in Figure 7 and Figure 8, the CGKS(refined one) has a similar resolution with the RKDG-$P^4$ method.

# 3 Conclusion

In this research, we systematically evaluate the performance of the RKDG method and the GKS in terms of accuracy, efficiency, and resolution. We demonstrate significant improvements in the efficiency of the GKS through the use of compact spatial reconstruction and a simplified third-order gas distribution method. Notably, GKS exhibits higher efficiency than the RKDG method in smooth flow regions. Importantly, GKS is capable of handling viscous flows without additional computational demands, whereas implementing viscous terms in the RKDG method requires further development, indicating a potentially higher efficiency of the CGKS for real-world viscous flow simulations. During the implementation of these methods, we encountered challenges in maintaining the stability of the RKDG method when using multi-resolution WENO limiters. The coefficients $\gamma_{\ell-1,\ell}$ and $\gamma_{\ell,\ell}$ for the limiters proved sensitive and required case-specific adjustments to achieve both robustness and accuracy in capturing discontinuous solutions. Furthermore, the multi-resolution scheme tends to incorrectly identify excessive extreme points in smooth regions, thereby attenuating extreme values. Our comparative analysis highlights the robustness of the CGKS and the high accuracy of the RKDG method in multi-dimensional scenarios. Thus, integrating the strengths of GKS's relaxed CFL conditions and DG's high accuracy, a hybrid scheme combining DG and CGKS with $h-p$ refinement emerges as a promising approach for effectively simulating flows in both smooth and discontinuous regions. This development is part of our ongoing research efforts.

# References

[1] Jun Zhu, Jianxian Qiu, and Chi-Wang Shu. High-order Runge-Kutta discontinuous Galerkin methods with a new type of multi-resolution WENO limiters. *Journal of Computational Physics*, 404:109105, 2020.

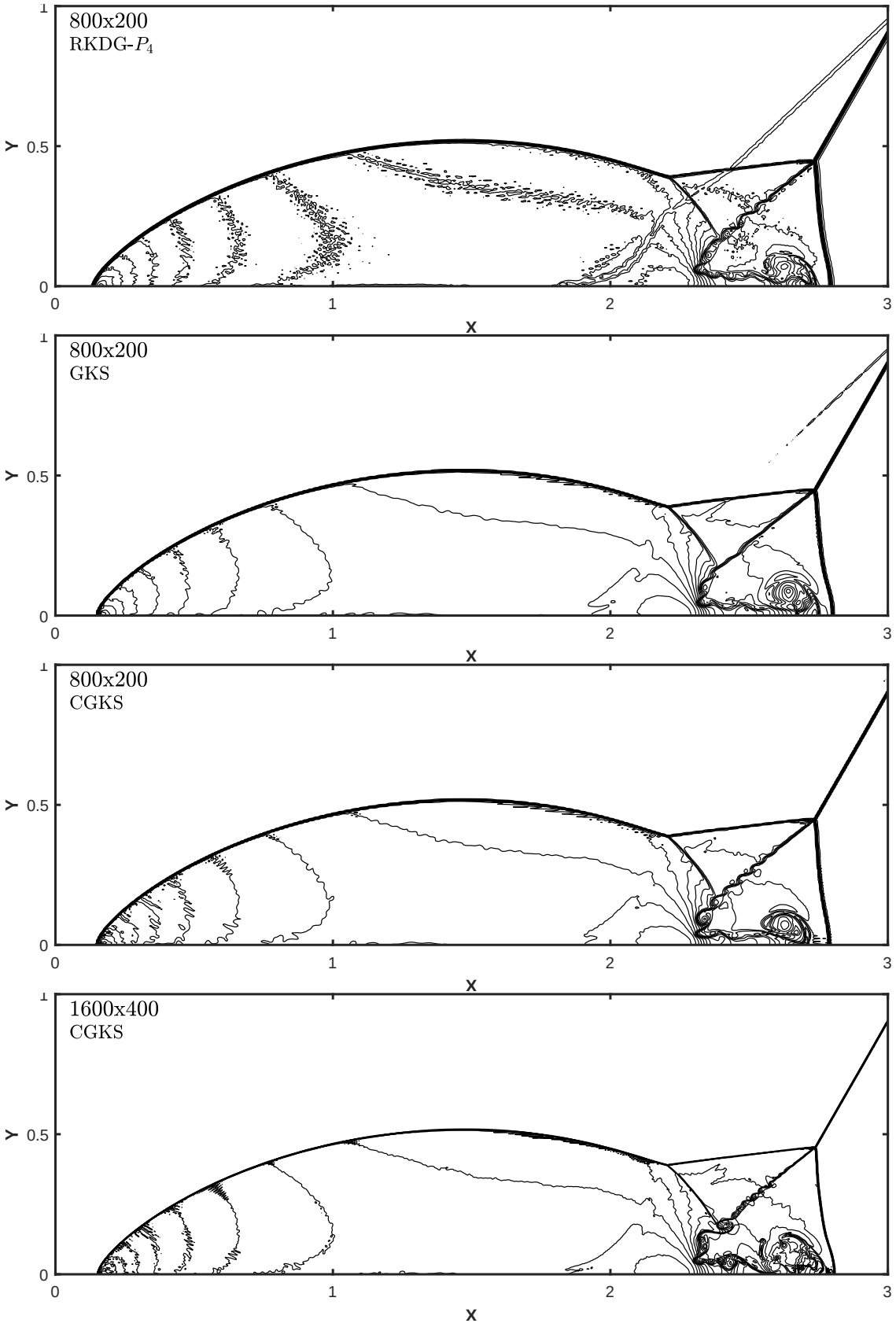


Figure 7: Double Mach problems: the density distributions at $t = 0.2s$. 30 equally spaced density contours from 1.5 to 21.5. From top to bottom: RKDG-$P^4$, fifth-order GKS, fifth-order CGKS, fifth-order CGKS(refined).

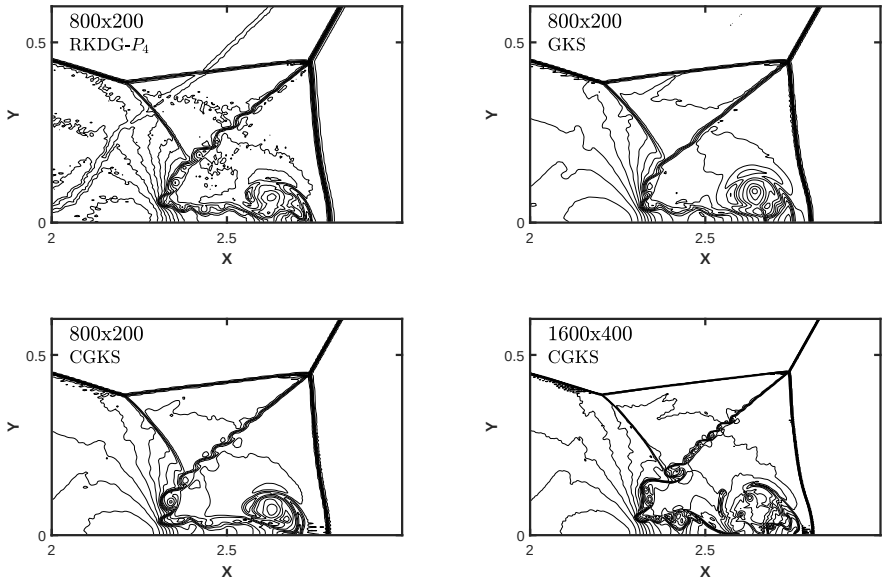


Figure 8: Double Mach problems: zoom-in pictures around the Mach stem. 30 equally spaced density contours from 1.5 to 21.5.From left to right and top to bottom: RKDG-$P^4$, fifth-order GKS, fifth-order CGKS, fifth-order CGKS(refined).

[2] Xing Ji, Liang Pan, Wei Shyy, and Kun Xu. A compact fourth-order gas-kinetic scheme for the Euler and Navier–Stokes equations. *Journal of Computational Physics*, 372:446–472, 2018.

[3] Kun Xu and Chang Liu. A paradigm for modeling and computation of gas dynamics. *Physics of Fluids*, 29(2):026101, 2017.

[4] John Charles Butcher. A history of Runge-Kutta methods. *Applied numerical mathematics*, 20(3):247–260, 1996.

[5] Chi-Wang Shu and Stanley Osher. Efficient implementation of essentially non-oscillatory shock-capturing schemes. *Journal of computational physics*, 77(2):439–471, 1988.

[6] Vladimir A Titarev and Eleuterio F Toro. Finite-volume WENO schemes for three-dimensional conservation laws. *Journal of Computational Physics*, 201(1):238–260, 2004.

[7] Timur Linde, Philip Roe, Timur Linde, and Philip Roe. Robust euler codes. In *13th computational fluid dynamics conference*, page 2098, 1997.

[8] Eleuterio F Toro, Michael Spruce, and William Speares. Restoration of the contact surface in the HLL-Riemann solver. *Shock waves*, 4:25–34, 1994.

[9] Paul Woodward and Phillip Colella. The numerical simulation of two-dimensional fluid flow with strong shocks. *Journal of computational physics*, 54(1):115–173, 1984.